nature photonics

REVIEW ARTICLE

PUBLISHED ONLINE: 31 JULY 2012 | DOI: 10.1038/NPHOTON.2012.175

Artificial photosynthesis for solar water-splitting

Yasuhiro Tachibana[1,2,3]*, Lionel Vayssieres[4]* and James R. Durrant[5]

Hydrogen generated from solar-driven water-splitting has the potential to be a clean, sustainable and abundant energy source. Inspired by natural photosynthesis, artificial solar water-splitting devices are now being designed and tested. Recent developments based on molecular and/or nanostructure designs have led to advances in our understanding of light-induced charge separation and subsequent catalytic water oxidation and reduction reactions. Here we review some of the recent progress towards developing artificial photosynthetic devices, together with their analogies to biological photosynthesis, including technologies that focus on the development of visible-light active hetero-nanostructures and require an understanding of the underlying interfacial carrier dynamics. Finally, we propose a vision for a future sustainable hydrogen fuel community based on artificial photosynthesis.

Solar-to-chemical energy conversion is the ultimate goal for scientists in the field of energy generation. This process does not emit greenhouse gases, and the chemical energy can be stored and used when required. Plants perform this conversion through natural photosynthesis (NPS)[1], in which oxygen and carbohydrates are produced from water and carbon dioxide using sunlight. The energy-conversion efficiency of NPS can reach around 7% under optimum conditions[2], although an efficiency of less than 1% is usually expected for agricultural crops over their entire lifecycle[1].

A potentially more controlled technology for the solar-to-chemical energy-conversion process is artificial photosynthesis (APS), which aims to emulate NPS using man-made materials. APS has been fascinating scientists in fields ranging from materials science to physical and inorganic chemistry. However, it remains a significant challenge to construct an efficient APS device capable of producing molecular fuels such as hydrogen at a scale and cost that can compete with fossil fuels. Significant advances in efficiency are required before such devices will be able to compete with conventional energy sources.

Photosynthetic reactions are determined primarily by three reaction processes: light-harvesting processes; charge generation and separation processes; and catalytic reaction processes. The overall efficiency is determined by the balance of thermodynamics and kinetics of these processes. In recent decades, intensive studies have been focused on further investigating the mechanisms involved in NPS. In particular, researchers recently revealed the structure of the oxygen-evolving site in photosystem II[3,4], thus providing new inspiration for designs of APS structures.

Over the past decade, fundamental progress has been made in developing novel material structures for water-splitting reactions — particularly in those that target an efficient oxygen-evolving catalyst for use in APS devices. Nanomaterial compositions and structures, including inorganic, molecular and hybrid organic/inorganic materials, have been explored to meet specific requirements such as a light-absorbing wavelength modification, photoinduced charge separation and a faster water-splitting reaction[5–13].

This Review summarizes the recent research trends of APS concepts and designs. In particular, we focus on the differences and similarities between NPS and APS, recent progress in design and structure, nanomaterial developments, and nanomaterial mechanisms and optimization. Novel nanomaterials have made significant improvements to water-splitting efficiencies. Concurrently, significant progress has been achieved in elucidating the mechanisms of water-splitting.

Comparison between natural and artificial photosynthesis

The light reaction of NPS occurs via a series of step-wise electron-transfer processes to create sufficient energy for water-splitting[1]. This process, known as the 'Z-scheme', is shown in Fig. 1a. Two photosystems — photosystem I (PSI) and photosystem II (PSII) — collect light energy through an assembly of light-harvesting chlorophylls and pump electrons to a higher electronic state (excitation) inside a reaction centre[14,15]. These photosystems are connected in series with an electron transfer chain. At the donor side of PSII, a water oxidation reaction occurs at a manganese calcium oxide cluster[3,16]. These processes ensure that the charge separation quantum efficiency is close to 100% under optimal conditions.

For APS systems, two different types of material structures are currently accepted. Figure 1b shows the first, which comprises a single light-excitation site attached to an electron donor on one side and an electron acceptor on the other. A dye molecule or visible-light-absorbing semiconductor is usually employed as the excitation site (chromophore). The absorption wavelengths are tuned by modifying the dye structure (the gap between the highest occupied molecular orbital (HOMO) and the lowest unoccupied molecular orbital (LUMO)) or designing the semiconductor's electronic structure (the bandgap). The electron donor material must meet two principal requirements. First, its energy level must be more negative than the excited state reduction potential of the chromophore, but more positive than the water oxidation potential. Second, the donor must be connected to the chromophore to induce a swift electron transfer reaction prior to decay of the chromophore excited state. Similar requirements must also be met for the electron acceptor: its potential energy level must be between the chromophore excited state oxidation potential and the water reduction potential. Co-catalysts are usually introduced to accelerate water-splitting reactions[17].

[1]School of Aerospace, Mechanical and Manufacturing Engineering, RMIT University, Bundoora, Victoria 3083, Australia. [2]Japan Science and Technology Agency (JST), PRESTO, 4-1-8 Honcho Kawaguchi, Saitama 332-0012, Japan. [3]Center for Advanced Science and Innovation (CASI), Osaka University, 2-1 Yamada-Oka, Suita, Osaka 565-0871, Japan. [4]International Research Center for Renewable Energy, State Key Laboratory of Multiphase Flow in Power Engineering, School of Energy and Power Engineering, Xian Jiaotong University, Xi'an 710049, China. [5]Department of Chemistry, Imperial College London, South Kensington Campus, London SW7 2AZ, UK. *e-mail: yasuhiro.tachibana@rmit.edu.au; lionelv@xjtu.edu.cn

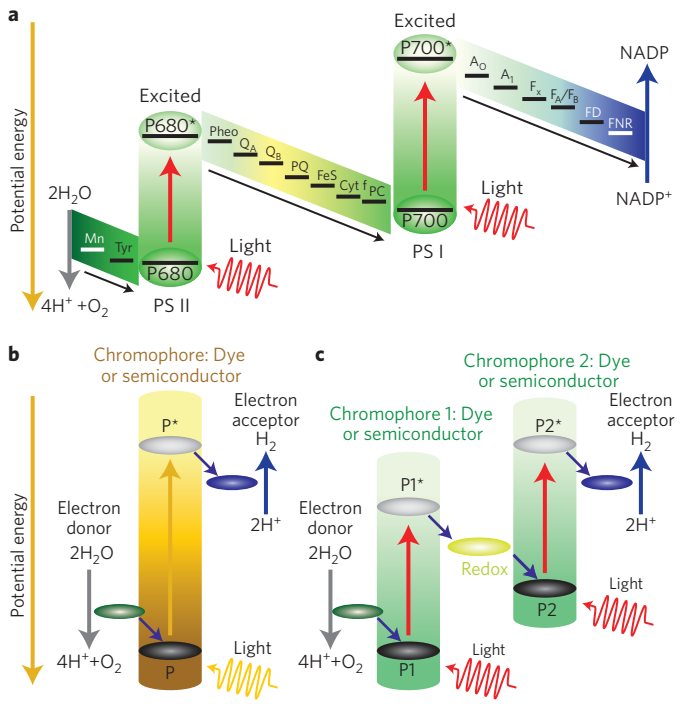

Figure 1 | Comparison between NPS and APS. a, NPS charge-separation processes, including type I and II reaction centres (simplified Z-scheme). P680: pigment (chlorophyll) that absorbs 680 nm light in photosystem II (PSII); P680*: the excited state of P680; P700: pigment (chlorophyll) that absorbs 700 nm light in photosystem I (PSI); P700*: the excited state of P700. Mn: manganese calcium oxide cluster; Tyr: tyrosine in PSII; Pheo: pheophytin, the primary electron acceptor of PSII; Q_A: primary plastoquinone electron acceptor; Q_B: secondary plastoquinone electron acceptor; PQ: plastoquinone; FeS: Rieske iron sulphur protein; Cyt. f: cytochrome f; PC: plastocyanin; A_0: primary electron acceptor of PSI; A_1: phylloquinone; F_X, F_A, F_B: three separate iron sulphur centres; FD: ferredoxin; FNR: nicotinamide adenine dinucleotide phosphate (NADP) reductase. This Z-scheme process is driven by the absorption of two photons, one at PSII and the other at PSI. Light absorption at PSII creates P680*, which provides an electron to reduce pheophytin, and the step-wise electron transfer occurs from pheophytin to $P700^+$ (the oxidizing species after the electron transfer from P700*). Following this initial electron transfer, $P680^+$ can oxidize tyrosine and subsequently the manganese calcium oxide cluster. Light absorption at PSI creates P700*, which provides an electron to reduce A_0 to FNR. A series of electron transfer pathways are indicated by black arrows. **b**,**c**, APS charge-separation processes: single-step reactions (**b**) and two-step (Z-scheme) reactions (**c**). P: chromophore of a single-step reaction system; P*: excited state of P; P1: the first chromophore of a two-step reaction system; P1*: excited state of P1; P2: second chromophore of a two-step reaction system; P2*: excited state of P2.

The main advantage of the single-step process is that the device structure is simple in comparison with the NPS Z-scheme. In addition to the chromophore, the material design can be focused on the electron acceptor site to optimize the hydrogen-producing process and on the donor site for the oxygen-evolving process. However, there are several drawbacks to the single-step process. First, material choice is limited because the chromophore excited-state reduction potential must be more positive than the water oxidation potential (+0.82 V relative to a normal hydrogen electrode at pH 7), and the excited-state oxidation potential must be more negative than the hydrogen evolution potential (−0.41 V relative to a normal hydrogen electrode at pH 7). Second, only a fraction of the sunlight can be utilized to initiate both hydrogen- and oxygen-evolution processes. Assuming such processes require 0.3 eV as a reaction driving force, and given that the energy difference between water oxidation and reduction potentials is 1.23 eV, the excitation energy required for the overall process is more than 1.83 eV (<677 nm).

The two-step process (Fig. 1c) is an alternative technique that is analogous to the NPS Z-scheme. Like the single-step process, the two-step process places requirements on the excited-state oxidation and reduction potentials, although these are less severe because two photons are employed to drive the overall water-splitting reaction. The electron transfer must be balanced through the electron-transfer relay materials between the chromophores. One advantage of the two-step process is that it can utilize lower energy sunlight (down to near-infrared wavelengths) and thus increases available choices for material combinations. As long as the excited-state oxidation potential at the oxygen-evolving site (P1* in Fig. 1c) is more negative than the excited state reduction potential at the hydrogen-evolving site (P2), there is no further potential requirement for these states. However, the overall system structure is more complex than that of the single-step process. For example, in the two-step process, it is more difficult to control the kinetic balance for the whole electron-transfer process without losing the energy through charge recombination reactions.

Designs and structures of artificial photosynthesis

Improving the efficiency of water-splitting reactions requires the device to be optimized in terms of its material selection and structure. Two types of device have been developed in this manner. The first was developed as an isolated photoactive species such as a molecular or semiconductor-particle-based device (Fig. 2a,b). Unfortunately, with such devices it is difficult to collect oxygen and hydrogen at separate regions, as these are likely to be generated simultaneously. However, separate gas collection could be achieved by employing the two-step process (Fig. 2c)[18,19]. For example, in Fig. 2c, oxygen is generated in one semiconductor system (left-hand side), while hydrogen is generated in the other (right-hand side). The second type of device is based on the integration of functional materials to form an electrode; that is, the oxygen- and hydrogen-evolution sites are separated and fabricated on different electrodes. In this case, the generated oxygen and hydrogen can be individually collected in separate containers. Here we discuss some examples of device structures recently developed by optimizing material functions that employ these strategies.

Molecular redox relays have been extensively studied as molecular devices since the 1970s[8,20–23]. Figure 2a shows a triad molecular structure[24] based on a single-step system with a porphyrin dye, which is similar to the chlorophyll structure in NPS, as the light-absorbing molecule. Electron transfer occurs from the porphyrin excited-state LUMO level (P*) to the fullerene (C_{60}), and from the carotenoid (C) to the porphyrin ground-state HOMO (P). Charge separation (forming $C^{\bullet+}$–P–$C_{60}^{\bullet-}$) completes on a picosecond timescale with a quantum yield of >95%, whereas charge recombination occurs on a sub-microsecond timescale. This design has been further improved by using light-harvesting molecules to capture light, and introducing a light-switching molecule to reduce photodamage[20,25].

Researchers have also developed a similar single-step system that uses semiconductor particles (Fig. 2b) or metal oxide electrodes (Fig. 2d). The major breakthrough was reported in 1972 by Honda and Fujishima, who used a TiO_2 film as a photoelectrode[26] but no co-catalysts on the TiO_2 surface. The photogenerated electron was separated from the hole at the TiO_2–electrolyte interface. Oxygen and hydrogen were generated at a TiO_2 electrode and at a platinum counter-electrode, respectively, in separate compartments inside the photoelectrochemical cell. Co-catalysts are often introduced to accelerate water-splitting reactions. Note that exact locations of the co-catalysts (such as in Fig. 2b) are rarely known, although some studies have identified the relationship between device morphology and the water-splitting activity[18,27]. Domen reported that the

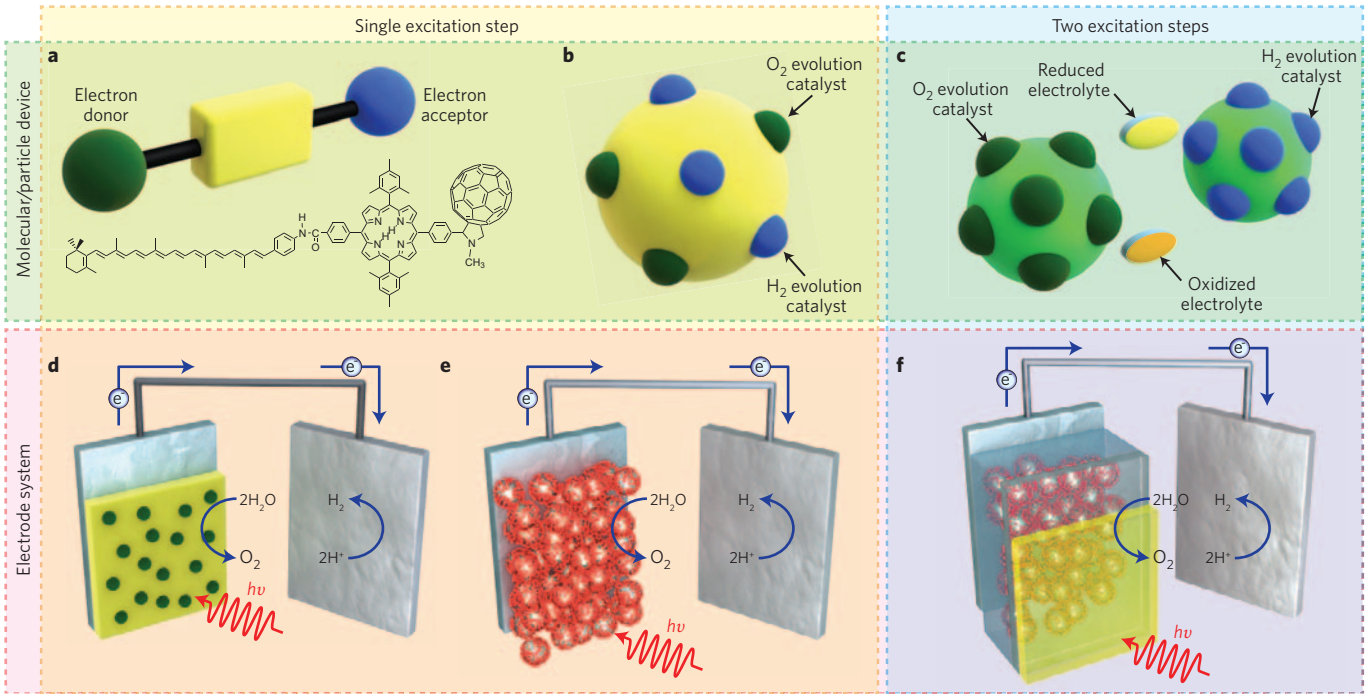

Figure 2 | Structural designs of APS reaction processes. a, Structure of the carotenoid–porphyrin–fullerene molecular dyad system. **b**, Single-step semiconductor particle with attached hydrogen- and oxygen-evolving co-catalysts. **c**, Two-step system: mixture of semiconductor particles with attached hydrogen- or oxygen-evolving co-catalyst and redox electrolyte couples. **d**, Single-excitation-step water-splitting cell, containing a semiconductor electrode with water oxidation co-catalysts and a counter-electrode to reduce water. **e**, Dye-sensitized transparent metal oxide water-splitting cell. **f**, Two-step tandem water-splitting cell. Inset of **a** reproduced with permission from ref. 24, © 2004 Wiley.

visible-light-absorbing semiconductor $(Ga_{1-x}Zn_x)(N_{1-x}O_x)$, with a co-catalyst, provides a water-splitting quantum efficiency of 2.5% at wavelengths of 420–440 nm (ref. 28).

Researchers have recently employed the combined structure of organic molecules and metal oxide nanoparticles as a single-step dye-sensitized water-splitting system. This configuration initiates (Fig. 2e) opportunities for the selection of a sensitizer dye with a different light absorption profile[29,30]. Mallouk *et al.* proposed a dye-sensitized TiO_2 water-splitting cell with hydrated iridium oxide nanoparticles as the oxygen-evolving catalyst[31]. Following electron injection from the excited ruthenium complex into a TiO_2 nanocrystal, the oxidation energy of the dye cation is used to split water using the iridium oxide attached to the dye. The injected electron in the TiO_2 is transferred to a platinum counter-electrode to produce hydrogen. Spiccia *et al.* also employed manganese as an 'Mn–oxo' cluster catalyst in a dye-sensitized water-splitting cell[32].

Several structures have been suggested for two-step water-splitting devices[19,33–36]. Abe, Domen and co-workers recently established two-step-based Z-scheme structures using an IO_3^-/I^- redox couple (Fig. 2c)[19,33]. The preferential attachment of redox species to the particular semiconductor surface selects either a water-splitting reaction or an electron-transfer reaction from I^-. Kudo *et al.* reported the formation of an aggregated structure comprising two different semiconducting nanomaterials, thus inducing swift electron-transfer processes between two light-absorbing semiconductors[37]. Tada *et al.* demonstrated a CdS–Au–TiO_2 Z-scheme system that contained a vectorial electron-transfer path[38]. The tandem cell configuration (Fig. 2f) is another favourable structure of the two-step system[34,35]. Grätzel *et al.* combined the oxygen-evolving electrode with the dye-sensitized TiO_2 electrode[34,35]. Researchers have also demonstrated water-splitting by employing multijunction photovoltaic devices coupled to oxidation and reduction catalysts; as for the Z-scheme, a multijunction device is required to generate a voltage sufficient for driving both the oxidation and reduction reactions[39–41].

Nanomaterial developments

Significant progress in the fabrication of nanomaterials has provided a plethora of novel and innovative hetero-nanostructures for solar water-splitting, with photocurrents ranging from microamperes to milliamperes per square centimetre. This rapid development has been the topic of many comprehensive reviews[6,18,30,36,42–49], perspectives[5,50], books[51–55] and book chapters[56]. Many reports focus on techniques for fabricating novel structures and devices, as well as the latest improvements of well-known large-bandgap semiconductors such as TiO_2 and ZnO, which exhibit high performances for solar water-splitting. Many new emerging systems, such as oxynitrides, tantalates and niobates, also show great potential.

From an academic standpoint, any functioning systems are necessary to understand and exploit the fundamental mechanisms and energetics involved in the water oxidation process. However, from a practical standpoint, and particularly for a cost-effective and sustainable large-scale implementation, very different issues must be addressed and fulfilled, including cost, abundance, low toxicity and long-term stability in water under strong illumination by concentrated solar irradiation. These crucial requirements suggest the use of cheap transition metals and naturally abundant chemical elements such as iron, titanium, zinc, carbon, nitrogen and sulphur.

It is also important to show the 'true' efficiency of the device; that is, its efficiency without the use of often costly or industrially irrelevant sacrificial agents. This demonstration would instead make use of the most abundant and geographically balanced free natural resource available on Earth — seawater. Although the market for photovoltaic devices grows daily, researchers have yet to develop modules for use in large-scale solar water-splitting facilities. The fabrication and testing of large systems, devices, modules and panels is of major importance. In addition, work so far has been limited mostly to n- or p-type photoanodes; very little attention has been paid to the cathode or the conducting substrate. An increase in Ohmic loss at larger areas requires the implementation of a

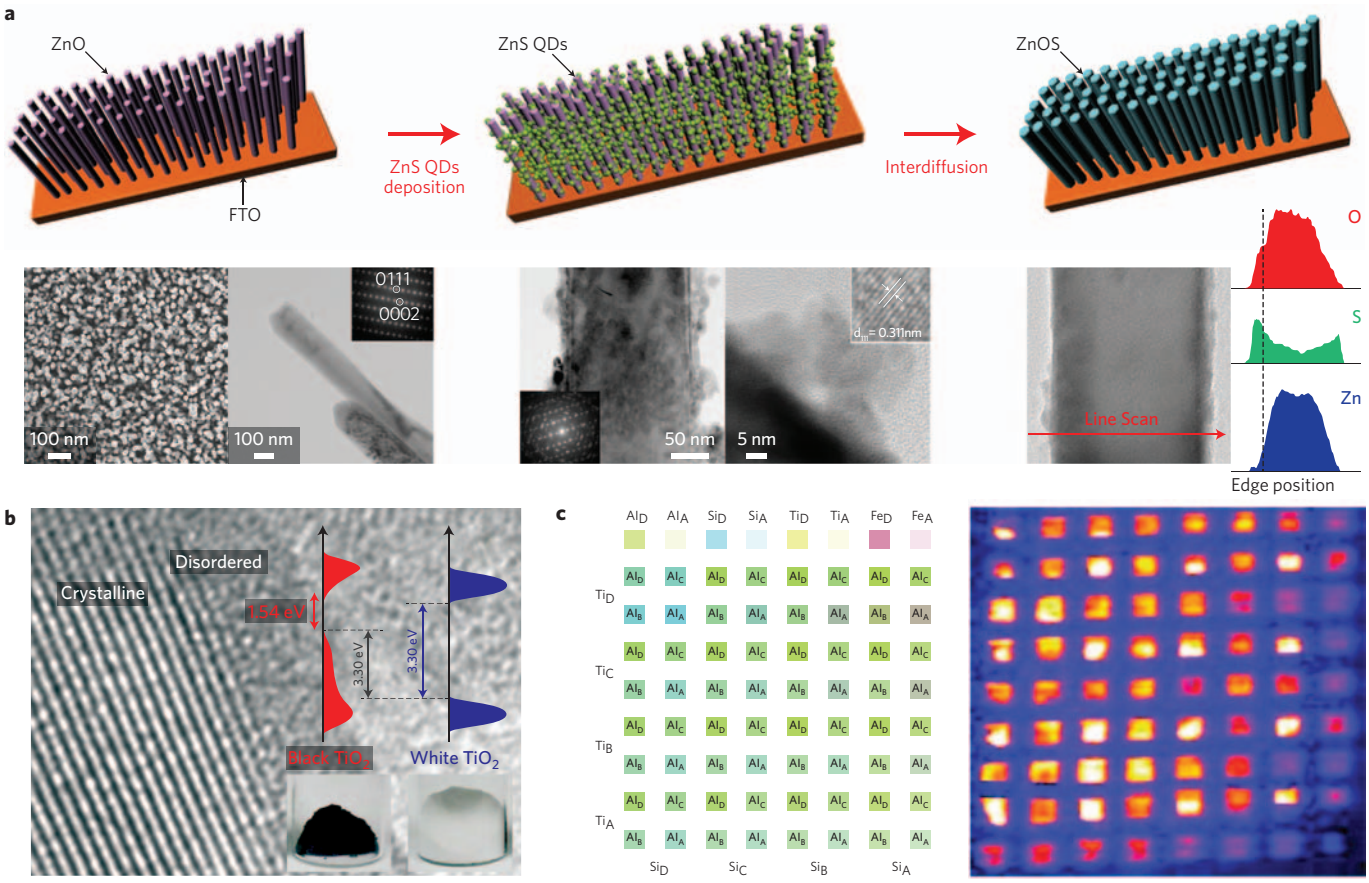

Figure 3 | New concepts of nanomaterial developments. a, Fabrication and characterization of a ZnOS nanowire array electrode on a fluorine-doped tin oxide (FTO) transparent conducting substrate. Top: the fabrication process. Bottom-left: scanning electron microscopy, transmission electron microscopy and selected area electron diffraction images of pristine ZnO nanowires. Bottom-centre: transmission electron microscopy images of ZnO nanowires covered in ZnS quantum dots. Bottom-right: elemental profiles extract from scanning transmission electron microscopy. **b**, High-resolution transmission electron microscopy images of black TiO_2 nanocrystals with a disordered outer layer. Inset: Density of states of black TiO_2 nanocrystals, as compared with that of unmodified TiO_2 nanocrystals. Image courtesy of S. S. Mao, adapted from ref. 71. **c**, Combinatorial method to investigate the incorporation of titanium, silicon and aluminium on the performance of α-Fe_2O_3 photoanodes, including the template used for the printed pattern (left) and the corresponding photocurrent maps (right). Image courtesy of Bruce A. Parkinson. Figure reproduced with permission from: **a**, ref. 70, © 2011 Wiley; **c**, ref. 75, © 2011 ACS.

conducting grid (usually made from silver or gold) to achieve the necessary conductivity, which raises the price of the device. New transparent conductive oxides have also been reported. The most striking of these are graphene-based, but their long-term stability has yet to be investigated. For the interface between a photoactive material and a transparent conductive oxide, researchers have demonstrated an order of magnitude increase in efficiency under sudden high-temperature annealing — an effect that has been attributed to atomic diffusion of tin and subsequent doping. From a structural point of view, the development of facet-selective reactivity, which is well-described for single crystals in heterogeneous catalysis, requires control over not only the material's shape, orientation and size, but also its surface and interfacial chemistry[57]. In addition, such local chemical control also enables the creation of chemical potential gradients of charges, which are necessary to maintain the dynamics under operating conditions. Recently, the importance of the interfacial electronic structure[58] and spontaneous electron enrichment[59] were shown to account quantitatively to the reported efficiency enhancement.

Recent approaches have utilized nanostructuring[60,61], quantum confinement[62], plasmonics[63–65], enhancement to the carrier dynamics, orbital engineering[66], up- and downconversion, and intermediate-band electronic structure[67]. Such strategies have proven successful, and a new generation of quantum-confined nanostructures with optimized bandgap and band edges tuned for efficient water-splitting has been fabricated. These quantum-dot-sensitized quantum-[68] and nano-rods[69] show significant efficiency improvement, particularly in the visible region of the solar spectrum (Fig. 3a)[70].

Hydrogenation is a very effective technique for fabricating efficient visible-wavelength-active semiconductor nanostructures in photoelectrochemical cells. Molecular hydrogen treatment is a well-known and powerful process for reducing oxides to metals, or for inducing mixed valency in an oxide structure in gaseous phase at elevated temperatures or electrochemically at room temperature by intercalation of protons in aqueous acidic solutions, which produces shallow donor levels. This process was recently applied to achieve a new concept called disorder engineering, in which disorders yield mid-gap states rather than shallow donor levels and hydrogen stabilizes the disorders. Mao and co-workers[71] reported high-pressure-treated H_2–TiO_2, which is black in colour while the formal oxidation of Ti remains at +IV (Fig. 3b). This is in contrast with typical mixed-valency compounds, also strongly coloured but where the lower oxidation state of the transition metal (for example, +III for Ti, +II for Fe and +V for W) is induced leading to the mixed-valency electron transfer responsible for the strong visible absorption.

Black TiO_2 nanocrystals also provide effective carrier-trapping sites for suppressing rapid recombination, and thus offer a new

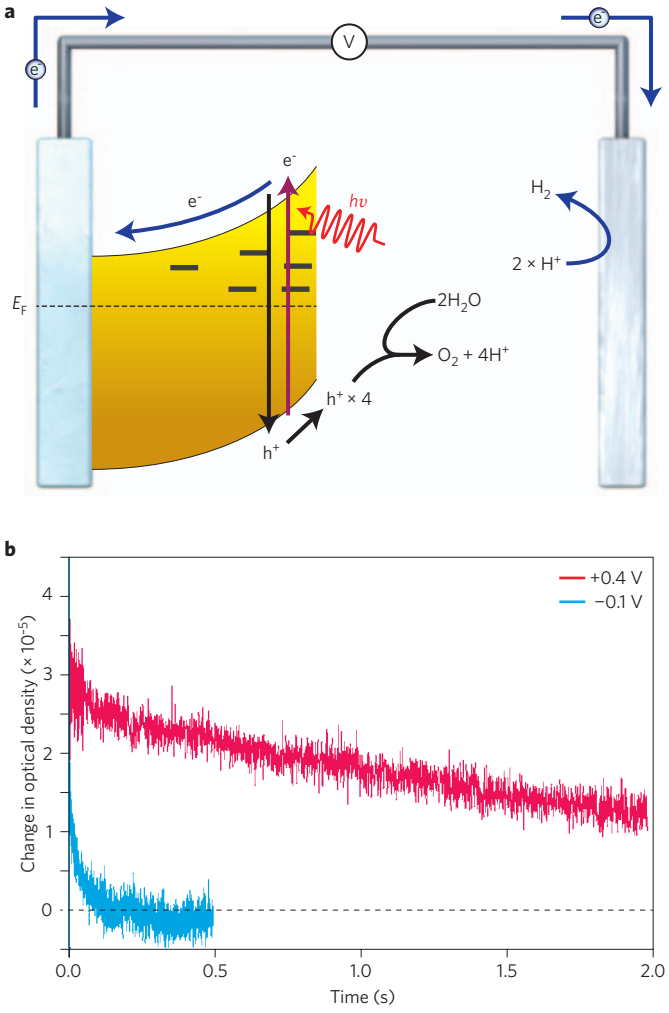

Figure 4 | Photo-induced charge separation and recombination of a semiconductor photoanode. a, Photoelectrochemical water-splitting cell employing a photoactive anodic electrode that induces a space-charge region at the semiconductor–solution interface. A photogenerated electron is separated from the interface and then consumed to generate hydrogen at the counter-electrode. A hole is generated at the interface and consumed for water oxidation reaction. **b**, Transient absorption data obtained for photogenerated holes in an α-Fe_2O_3 photoanode under a bias of −0.1 or +0.4 V relative to Ag/AgCl (ref. 91). Rapid decay under negative bias is due to electron–hole recombination. Under positive bias, the formation of a space-charge layer results in the generation of long-lived holes, which can oxidize water on a timescale of around 1 s.

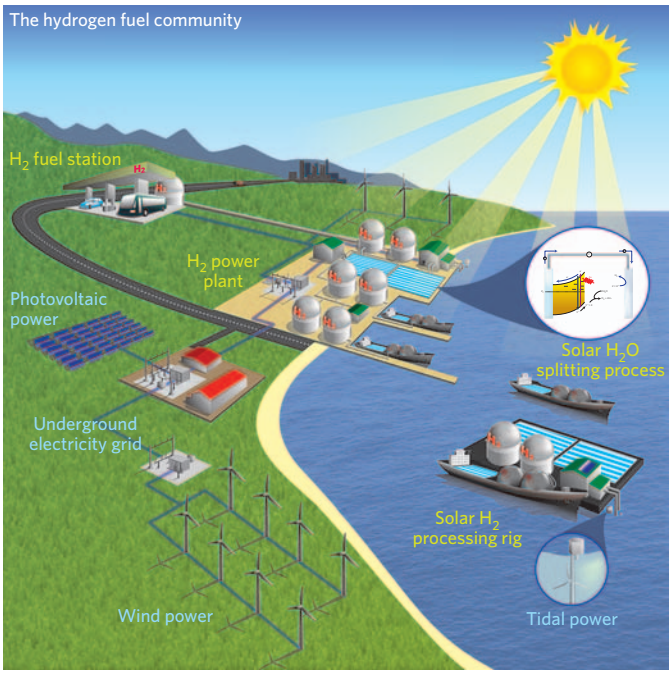

Figure 5 | Vision of a sustainable hydrogen fuel community based on APS. Hydrogen is produced from an APS solar water-splitting power plant using seawater on floating ports, tankers and seashore plants. Electricity needed to operate such an infrastructure is provided by renewable energy sources such as photovoltaic, wind and tidal power.

path towards photocatalysts that may offer not only a substantially enhanced photocatalytic activity under solar radiation, but also the desired stability for practical implementation. The concept of disorder engineering opens a new direction for altering optical absorption and carrier transport in semiconductor nanostructures. It is anticipated that combining disorder engineering with elemental doping could be used to overcome the lack of absorption in the visible range and may also reduce the limiting effects of bandgap energy and carrier recombination for many wide-bandgap materials that traditionally have not been considered for solar-related applications. Indeed, inspired by Mao's work, Zhang and collaborators reported H_2–TiO_2 nanowire arrays[72] and recently introduced H_2–WO_3, enabling the generation of oxygen even at neutral pH[73]. Previous operating conditions, in contrast, required the use of highly concentrated acid.

The past decade has seen the resurgence of α-Fe_2O_3 (hematite) — an abundant natural mineral — alongside the considerable efforts put into fabricating and discovering novel structures by experimental techniques such as high-throughput combinatorial chemistry[74,75] (Fig. 3c) or by calculation methods[76]. At the beginning of the twenty-first century, the Lindquist group in Sweden demonstrated that hematite designed as vertically oriented nanorods, in which the rod diameter matched the minority carrier diffusion length, could provide a quantum efficiency of up to 56% at a wavelength of 350 nm (refs 77,78). Since then, owing to the relentless efforts and ingenuity of many groups around the world[61,75,79–81], the efficiency of hematite-based nanostructures has increased exponentially to more than 3 mA cm^{-2}. This rapid development has even been compared to that of silicon-based solar cells in the 1970s[80]. Hematite exhibits the most important properties for a solar water-splitting material — price, stability, efficiency and non-toxicity — and therefore has significant potential providing that industrial (and potentially environmental[82]) issues are appropriately tackled[2,83–85].

Charge carrier dynamics

A key challenge for APS systems is to utilize the electron–hole pairs generated by photon absorption to drive the multi-electron chemistry required for fuel synthesis. In general, and in particular for the key reaction of water oxidation, this multi-electron chemistry is both thermodynamically challenging and kinetically slow. It is widely recognized that there is a significant mismatch between the nanosecond (or shorter) lifetimes of electron–hole pairs generated by photon absorption in a material and the timescales for the interfacial redox reactions required for water oxidation or proton/carbon dioxide reduction. As a consequence, electron–hole recombination is a major loss pathway that limits the quantum efficiency of photosynthetic systems. In NPS reaction centres, a molecular redox relay is employed to separate spatially photogenerated electrons and holes (Fig. 1a), thereby reducing recombination losses and, for example, enabling the accumulation of multiple oxidizing equivalents on the oxygen-evolving catalyst required for water oxidation. It should be noted that achieving this spatial separation often requires a

significant energy loss, corresponding, for the NPS reaction centres, to up to half the energy of the initially generated chlorophyll excited state, as illustrated in Fig. 1a. For inorganic photovoltaic devices, a p–n junction is often employed to spatially separate electrons and holes, thereby reducing minority carrier recombination losses.

For APS systems, a range of techniques have the potential to reduce electron–hole recombination losses. These include nanostructuring the photoactive materials to reduce the distance electron and holes must travel before reaching surface-reactive sites; the use of interfacial space regions to enable localization of single charge carriers at the material interface; the use of co-catalysts to accelerate interfacial oxidation–reduction kinetics; and the use of heterojunction structures to achieve spatial separation of electrons and holes. The preceding section discussed several examples in which these approaches have been shown to enhance the overall energy-conversion efficiency. Figure 4a illustrates a photoelectrochemical water-splitting cell that uses a photoactive electrode to induce a space charge region at the semiconductor–solution interface. A photogenerated electron is separated from the interface, moved through the semiconductor and collected at the back contact electrode. A corresponding hole is accumulated at the interface and consumed for water oxidation. In this context, the role of dopants is an important consideration. Water oxidation photoelectrodes are typically made from doped n-type semiconductors to avoid resistive losses associated with electron collection by the back contact. However, n-doping also has the effect of reducing the lifetime of the photogenerated holes — the minority carriers — due to faster electron–hole recombination. To date, there have been relatively few quantitative studies into the charge carrier dynamics in APS systems, how these dynamics are related to material design, and how they impact the water-splitting efficiency.

Most kinetic studies of charge carrier dynamics in APS systems have been undertaken for molecular energy and electron-transfer relays such as the triad structure (Fig. 2a). Such systems, which have typically been studied as suspensions in dilute solution, show close parallels with the function of NPS reaction centres. Transient spectroscopic studies have provided a detailed understanding of the charge carrier dynamics in such systems, as well as the relationships between electron-transfer rate constants and the quantum yields, energetics and lifetimes of charge-separated states[20]. In contrast, there have been relatively few studies into heterogeneous systems such as photoanodes and nanoparticle suspensions, and systems incorporating catalytic centres[86,87]. For photoanodes, most studies have involved photoelectrochemical techniques such as impedance analyses, which are now leading to increasingly detailed models of photoelectrode function[88,89]. In heterogeneous systems, a particular challenge is that electron–hole recombination is a bimolecular process; its dynamics often depend nonlinearly on the charge carrier density and so cannot be described with a single time constant. Such recombination dynamics have been most widely studied using transient optical spectroscopy techniques. Some studies have focused on correlating the ultrafast dynamics of electron–hole recombination with photoelectrode performance[90], whereas others have addressed slower (nanosecond to millisecond) timescales, where charge trapping in intraband states often has a significant impact on the observed dynamics[91,92].

Titania is the heterogeneous photocatalytic system in which charge carrier dynamics have been studied in great detail, due in part to the widespread use of this material in APS systems and dye-sensitized solar cells[93,94], as well as for the photocatalytic decomposition of pollutants[95]. More recently, attention has turned to lower-bandgap systems such as hematite. Several studies, such as that shown in Fig. 4b, have indicated that the rate constant for water oxidation by hematite holes is rather slow (around 1 s^{-1}). Such slow kinetics are a significant issue when considering the efficiency of water oxidation[88,91,96].

Perspectives

APS has the potential to provide significant economic, environmental and social benefits, providing that solar energy-conversion efficiencies increase and production/operating costs decrease. Researchers have suggested that the maximum solar energy-conversion efficiency of the water-splitting reaction could be comparable to that achievable with a photovoltaic device[97,98], thus indicating that theoretical efficiencies for single-junction devices could approach 31% under 1 Sun (1 kW m^{-2}) at AM1.5G illumination[36,97]. Over the past few years, research efforts have resulted in the emergence of new generations of visible-light-active hetero-nanostructures that combine advances in nanoscience such as confinements effects, innovative novel materials composition such as titanates, tantalates and niobates, and low-cost fabrication techniques such as hydrothermal and chemical vapour deposition. All of these developments represent excellent candidates for efficient hydrogen generation by APS, and some operate without any additives and/or at reduced or zero bias. However, to comply with the challenging requirements of economically viable industrial production of hydrogen by solar water-splitting, many issues are still yet to be addressed, including long-term stability in water and under concentrated illumination, toxicity to individuals and the environment, manufacturing costs and standardization[99]. A further challenge is translating laboratory-scale academic research into scalable, manufacturable technologies, including considerations of packaging, large-area processing and outdoor testing. New generations of APS devices that employ either direct photoreactors or spatially separated photovoltaic cells and electrolysers may render solar hydrogen generation commercially viable, thus enabling a sustainable hydrogen economy. For example, the US department of Energy has said that the price of hydrogen must reach US$2–3 kg^{-1} (including production, delivery and dispensing) before it can compete with gasoline for use in passenger vehicles. Figure 5 illustrates the implementation of a sustainable solar water-splitting power plant for safe, clean and efficient hydrogen production and utilization. This vision involves the assistance of commercially available renewable energy sources such as wind, solar and tidal to assist in powering the plant and thus reducing operating costs. The facility could be implemented in any seashore or off-shore location where seawater can be pumped and filtered, including platforms, tankers and floating or fixed ports. This seawater would be injected into APS modules for the generation of hydrogen, which can then be transported to fuelling stations with limited environmental issues relating to the implementation of large-area power stations[82,100]. After all, the most abundant, geographically balanced and freely available resources on this blue planet are sunlight and seawater.

References

1. Barber, J. Photosynthetic energy conversion: Natural and artificial. *Chem. Soc. Rev.* **38,** 185–196 (2009).
2. Blankenship, R. E. *et al.* Comparing photosynthetic and photovoltaic efficiencies and recognizing the potential for improvement. *Science* **332,** 805–809 (2011).
3. Umena, Y., Kawakami, K., Shen, J.-R. & Kamiya, N. Crystal structure of oxygen-evolving Photosystem II at a resolution of 1.9 Å. *Nature* **473,** 55–60 (2011).
4. Barber, J. Crystal structure of the oxygen-evolving complex of Photosystem II. *Inorg. Chem.* **47,** 1700–1710 (2008).
5. Kronawitter, C. X. *et al.* A perspective on solar-driven water splitting with all-oxide hetero-nanostructures. *Energ. Environ. Sci.* **4,** 3889–3899 (2011).
6. Maeda, K. & Domen, K. Photocatalytic water splitting: Recent progress and future challenges. *J. Phys. Chem. Lett.* **1,** 2655–2661 (2010).
7. Tachibana, Y., Umekita, K., Otsuka, Y. & Kuwabata, S. Charge recombination kinetics at an *in-situ* chemical bath-deposited CdS/Nanocrystalline TiO_2 Interface. *J. Phys. Chem. C* **113,** 6852–6858 (2009).
8. Wasielewski, M. R. Self-assembly strategies for integrating light harvesting and charge separation in artificial photosynthetic systems. *Acc. Chem. Res.* **42,** 1910–1921 (2009).

9. Yin, Q. *et al.* A fast soluble carbon-free molecular water oxidation catalyst based on abundant metals. *Science* **328,** 342–345 (2010).
10. Kanan, M. W. & Nocera, D. G. *In-situ* formation of an oxygen-evolving catalyst in neutral water containing phosphate and Co^{2+}. *Science* **321,** 1072–1075 (2008).
11. Lewis, N. S. & Nocera, D. G. Powering the planet: Chemical challenges in solar energy utilization. *Proc. Natl Acad. Sci. USA* **103,** 15729–15735 (2006).
12. Sivasankar, N., Weare, W. W. & Frei, H. Direct observation of a hydroperoxide surface intermediate upon visible light-driven water oxidation at an Ir Oxide nanocluster catalyst by rapid-scan FT-IR spectroscopy. *J. Am. Chem. Soc.* **133,** 12976–12979 (2011).
13. Nocera, D. G. The artificial leaf. *Acc. Chem. Res.* **45,** 767–776 (2012).
14. Fleming, G. R., Schlau-Cohen, G. S., Amarnath, K. & Zaks, J. Design principles of photosynthetic light-harvesting. *Faraday Discuss.* **155,** 27–41 (2012).
15. Herek, J. L., Wohlleben, W., Cogdell, R. J., Zeidler, D. & Motzkus, M. Quantum control of energy flow in light harvesting. *Nature* **417,** 533–535 (2002).
16. Siegbahn, P. E. M. Structures and energetics for O_2 formation in Photosystem II. *Acc. Chem. Res.* **42,** 1871–1880 (2009).
17. Limburg, J. *et al.* A functional model for O–O bond formation by the O_2-evolving complex in Photosystem II. *Science* **283,** 1524–1527 (1999).
18. Kudo, A. & Miseki, Y. Heterogeneous photocatalyst materials for water splitting. *Chem. Soc. Rev.* **38,** 253–278 (2009).
19. Abe, R. Recent progress on photocatalytic and photoelectrochemical water splitting under visible light irradiation. *J. Photochem. Photobiol. C* **11,** 179–209 (2010).
20. Gust, D., Moore, T. A. & Moore, A. L. Solar fuels via artificial photosynthesis. *Acc. Chem. Res.* **42,** 1890–1898 (2009).
21. Hammarström, L. & Styring, S. Proton-coupled electron transfer of tyrosines in Photosystem II and model systems for artificial photosynthesis: The role of a redox-active link between catalyst and photosensitizer. *Energ. Environ. Sci.* **4,** 2379–2388 (2011).
22. Gonzalez-Rodriguez, D. *et al.* Activating multistep charge-transfer processes in fullerene–subphthalocyanine–ferrocene molecular hybrids as a function of π–π orbital overlap. *J. Am. Chem. Soc.* **132,** 16488–16500 (2010).
23. Fukuzumi, S. & Ohkubo, K. Assemblies of artificial photosynthetic reaction centers. *J. Mater. Chem.* **22,** 4575–4587 (2012).
24. Kodis, G., Liddell, P. A., Moore, A. L., Moore, T. A. & Gust, D. Synthesis and photochemistry of a carotene–porphyrin–fullerene model photosynthetic reaction center. *J. Phys. Org. Chem.* **17,** 724–734 (2004).
25. Gust, D., Moore, T. A. & Moore, A. L. Realizing artificial photosynthesis. *Faraday Discuss.* **155,** 9–26 (2012).
26. Fujishima, A. & Honda, K. Electrochemical photolysis of water at a semiconductor electrode. *Nature* **238,** 37–38 (1972).
27. Kato, H., Asakura, K. & Kudo, A. Highly efficient water splitting into H_2 and O_2 over lanthanum-doped $NaTaO_3$ photocatalysts with high crystallinity and surface nanostructure. *J. Am. Chem. Soc.* **125,** 3082–3089 (2003).
28. Maeda, K. *et al.* Photocatalyst releasing hydrogen from water. *Nature* **440,** 295 (2006).
29. Reisner, E., Powell, D. J., Cavazza, C., Fontecilla-Camps, J. C. & Armstrong, F. A. Visible light-driven H_2 production by hydrogenases attached to dye-sensitized TiO_2 nanoparticles. *J. Am. Chem. Soc.* **131,** 18457–18466 (2009).
30. Chen, X., Shen, S., Guo, L. & Mao, S. S. Semiconductor-based photocatalytic hydrogen generation. *Chem. Rev.* **110,** 6503–6570 (2010).
31. Youngblood, W. J. *et al.* Photoassisted overall water splitting in a visible light-absorbing dye-sensitized photoelectrochemical cell. *J. Am. Chem. Soc.* **131,** 926–927 (2009).
32. Brimblecombe, R., Koo, A., Dismukes, G. C., Swiegers, G. F. & Spiccia, L. Solar-driven water oxidation by a bio-inspired manganese molecular catalyst. *J. Am. Chem. Soc.* **132,** 2892–2894 (2010).
33. Maeda, K., Higashi, M., Lu, D., Abe, R. & Domen, K. Efficient nonsacrificial water splitting through two-step photoexcitation by visible light using a modified oxynitride as a hydrogen evolution photocatalyst. *J. Am. Chem. Soc.* **132,** 5858–5868 (2010).
34. Grätzel, M. Photoelectrochemical cells. *Nature* **414,** 338–344 (2001).
35. Duret, A. & Grätzel, M. Visible light-induced water oxidation on mesoscopic alpha-Fe_2O_3 films made by ultrasonic spray pyrolysis. *J. Phys. Chem. B* **109,** 17184–17191 (2005).
36. Walter, M. G. *et al.* Solar water splitting cells. *Chem. Rev.* **110,** 6446–6473 (2010).
37. Sasaki, Y., Nemoto, H., Saito, K. & Kudo, A. Solar water splitting using powdered photocatalysts driven by Z-schematic interparticle electron transfer without an electron mediator. *J. Phys. Chem. C* **113,** 17536–17542 (2009).
38. Tada, H., Mitsui, T., Kiyonaga, T., Akita, T. & Tanaka, K. All-solid-state Z-scheme in CdS-Au-TiO_2 three-component nanojunction system. *Nature Mater.* **5,** 782–786 (2006).
39. Reece Steven, Y. *et al.* Wireless solar water splitting using silicon-based semiconductors and earth-abundant catalysts. *Science* **334,** 645–648 (2011).
40. Khaselev, O. & Turner, J. A. A monolithic photovoltaic–photoelectrochemical device for hydrogen production via water splitting. *Science* **280,** 425–427 (1998).
41. Rocheleau, R. E., Miller, E. L. & Misra, A. High-efficiency photoelectrochemical hydrogen production using multijunction amorphous silicon photoelectrodes. *Energy Fuels* **12,** 3–10 (1998).
42. Kubacka, A., Fernandez-Garcia, M. & Colon, G. Advanced nanoarchitectures for solar photocatalytic applications. *Chem. Rev.* **112,** 1555–1614 (2012).
43. Valdes, A. *et al.* Solar hydrogen production with semiconductor metal oxides: New directions in experiment and theory. *Phys. Chem. Chem. Phys.* **14,** 49–70 (2012).
44. Xing, J., Fang, W. Q., Zhao, H. J. & Yang, H. G. Inorganic photocatalysts for overall water splitting. *Chem. Asian J.* **7,** 642–657 (2012).
45. Shen, S., Shi, J., Guo, P. & Guo, L. Visible-light-driven photocatalytic water splitting on nanostructured semiconducting materials. *Int. J. Nanotechnol.* **8,** 523–591 (2011).
46. Osterloh, F. E. & Parkinson, B. A. Recent developments in solar water-splitting photocatalysis. *MRS Bull.* **36,** 17–22 (2011).
47. Tributsch, H. Photovoltaic hydrogen generation. *Int. J. Hydrogen Energ.* **33,** 5911–5930 (2008).
48. Sahaym, U. & Norton, M. G. Advances in the application of nanotechnology in enabling a 'hydrogen economy'. *J. Mater. Sci.* **43,** 5395–5429 (2008).
49. Henderson, M. A. A surface science perspective on TiO_2 photocatalysis. *Surf. Sci. Rep.* **66,** 185–297 (2011).
50. Sun, J., Zhong, D. K. & Gamelin, D. R. Composite photoanodes for photoelectrochemical solar water splitting. *Energ. Environ. Sci.* **3,** 1252–1261 (2010).
51. Vayssieres, L. (ed.) *On Solar Hydrogen & Nanotechnology* (Wiley, 2009).
52. Zini, G. & Tartarini, P. *Solar Hydrogen Energy Systems: Science and Technology for the Hydrogen Economy* (Springer, 2012).
53. Grimes, C. A. *Light, Water, Hydrogen: The Solar Generation of Hydrogen by Water Photoelectrolysis* (Springer, 2007).
54. Rajeshwar, K., McConnell, R. & Licht, S. (eds) *Solar Hydrogen Generation: Toward a Renewable Energy Future* (Springer, 2010).
55. Guo, J. & Chen, X. *Solar Hydrogen Generation: Transition Metal Oxides in Water Photoelectrolysis* (McGraw Hill, 2012).
56. Chouhan, N. *Photoelectrochemical cells for hydrogen generation* in Electrochemical Technologies for Energy Storage and Conversion (ed. Zhang, J. Z.) 539–597 (Wiley, 2011).
57. Vayssieres, L. On the effect of nanoparticle size on water-oxide interfacial chemistry. *J. Phys. Chem. C* **113,** 4733–4736 (2009).
58. Kronawitter, C. X. *et al.* TiO_2–SnO_2:F interfacial electronic structure investigated by soft X-ray absorption spectroscopy. *Phys. Rev. B* **85,** 125109 (2012).
59. Kronawitter, C. X. *et al.* Electron enrichment in 3d transition metal oxide hetero-nanostructures. *Nano. Lett.* **11,** 3855–3861 (2011).
60. Boettcher, S. W. *et al.* Energy-conversion properties of vapor–liquid–solid-grown silicon wire-array photocathodes. *Science* **327,** 185–187 (2010).
61. Kay, A., Cesar, I. & Grätzel, M. New benchmark for water photooxidation by nanostructured alpha-Fe_2O_3 films. *J. Am. Chem. Soc.* **128,** 15714–15721 (2006).
62. Vayssieres, L., Persson, C. & Guo, J. H. Size effect on the conduction band orbital character of anatase TiO_2 nanocrystals. *Appl. Phys. Lett.* **99,** 183101 (2011).
63. Linic, S., Christopher, P. & Ingram, D. B. Plasmonic-metal nanostructures for efficient conversion of solar to chemical energy. *Nature Mater.* **10,** 911–921 (2011).
64. Warren, S. C. & Thimsen, E. Plasmonic solar water splitting. *Energ. Environ. Sci.* **5,** 5133–5146 (2012).
65. Solarska, R., Krolikowska, A. & Augustynski, J. Silver nanoparticle induced photocurrent enhancement at WO_3 photoanodes. *Angew. Chem. Int. Ed.* **49,** 7980–7983 (2010).
66. Vayssieres, L. *et al.* One-dimensional quantum-confinement effect in α-Fe_2O_3 ultrafine nanorod arrays. *Adv. Mater.* **17,** 2320–2323 (2005).
67. Luque, A., Marti, A. & Stanley, C. Understanding intermediate-band solar cells. *Nature Photon.* **6,** 146–152 (2012).
68. Vayssieres, L. (ed.) *On Solar Hydrogen & Nanotechnology* 523–558 (Wiley, 2009).
69. Chen, H. M. *et al.* Quantum dot monolayer sensitized ZnO nanowire-array photoelectrodes: True efficiency for water splitting. *Angew. Chem. Int. Ed.* **49,** 5966–5969 (2010).
70. Chen, H. M. *et al.* A new approach to solar hydrogen production: A ZnO–ZnS solid solution nanowire array photoanode. *Adv. Energy Mater.* **1,** 742–747 (2011).
71. Chen, X., Liu, L., Yu, P. Y. & Mao, S. S. Increasing solar absorption for photocatalysis with black hydrogenated titanium dioxide nanocrystals. *Science* **331,** 746–750 (2011).

72. Wang, G. *et al.* Hydrogen-treated TiO_2 nanowire arrays for photoelectrochemical water splitting. *Nano. Lett.* **11,** 3026–3033 (2011).
73. Wang, G. *et al.* Hydrogen-treated WO_3 nanoflakes show enhanced photostability. *Energ. Environ. Sci.* **5,** 6180–6187 (2011).
74. Mao, S. S. High throughput combinatorial screening of semiconductor materials. *Appl. Phys. A* **105,** 283–288 (2011).
75. He, J. & Parkinson, B. A. Combinatorial investigation of the effects of the incorporation of Ti, Si, and Al on the performance of α-Fe_2O_3 photoanodes. *ACS Comb. Sci.* **13,** 399–404 (2011).
76. Greeley, J., Jaramillo, T. F., Bonde, J., Chorkendorff, I. B. & Norskov, J. K. Computational high-throughput screening of electrocatalytic materials for hydrogen evolution. *Nature Mater.* **5,** 909–913 (2006).
77. Beermann, N., Vayssieres, L., Lindquist, S.-E. & Hagfeldt, A. Photoelectrochemical studies of oriented nanorod thin films of hematite. *J. Electrochem. Soc.* **147,** 2456–2461 (2000).
78. Vayssieres, L., Beermann, N., Lindquist, S.-E. & Hagfeldt, A. Controlled aqueous chemical growth of oriented three-dimensional crystalline nanorod arrays: Application to iron (III) oxides. *Chem. Mater.* **13,** 233–235 (2001).
79. Lin, Y., Yuan, G., Sheehan, S., Zhou, S. & Wang, D. Hematite-based solar water splitting: Challenges and opportunities. *Energ. Environ. Sci.* **4,** 4862–4869 (2011).
80. Sivula, K., Le Formal, F. & Grätzel, M. Solar water splitting: Progress using hematite (α-Fe_2O_3) photoelectrodes. *Chem. Sus. Chem.* **4,** 432–449 (2011).
81. Cummings, C. Y., Marken, F., Peter, L. M., Wijayantha, K. G. U. & Tahir, A. A. New insights into water splitting at mesoporous α-Fe_2O_3 films: A study by modulated transmittance and impedance spectroscopies. *J. Am. Chem. Soc.* **134,** 1228–1234 (2012).
82. Haederle, M. Solar showdown in *Miller-McCune* (May/June 2011).
83. Braham, R. J. & Harris, A. T. Review of major design and scale-up considerations for solar photocatalytic reactors. *Ind. Eng. Chem. Res.* **48,** 8890–8905 (2009).
84. Christopher, K. & Dimitrios, R. A review on exergy comparison of hydrogen production methods from renewable energy sources. *Energ. Environ. Sci.* **5,** 6640–6651 (2012).
85. Dahl, S. & Chorkendorff, I. Solar-fuel generation. Towards practical implementation. *Nature Mater.* **11,** 100–101 (2012).
86. Lomoth, R. *et al.* Mimicking the electron donor side of Photosystem II in artificial photosynthesis. *Photosynth. Res.* **87,** 25–40 (2006).
87. Jiao, F. & Frei, H. Nanostructured cobalt and manganese oxide clusters as efficient water oxidation catalysts. *Energ. Environ. Sci.* **3,** 1018–1027 (2010).
88. Peter, L. M., Wijayantha, K. G. U. & Tahir, A. A. Kinetics of light-driven oxygen evolution at alpha-Fe_2O_3 electrodes. *Faraday Discuss.* **155,** 309–322 (2012).
89. Le Formal, F. *et al.* Passivating surface states on water splitting hematite photoanodes with alumina overlayers. *Chem. Sci.* **2,** 737–743 (2011).
90. Zhang, J. Z. Challenges and opportunities in light and electrical energy conversion. *J. Phys. Chem. Lett.* **2,** 1351–1352 (2011).
91. Pendlebury, S. R. *et al.* Dynamics of photogenerated holes in nanocrystalline alpha-Fe_2O_3 electrodes for water oxidation probed by transient absorption spectroscopy. *Chem. Commun.* **47,** 716–718 (2011).
92. Wang, X. *et al.* Trap states and carrier dynamics of TiO_2 studied by photoluminescence spectroscopy under weak excitation condition. *Phys. Chem. Chem. Phys.* **12,** 7083–7090 (2010).
93. Tachibana, Y., Moser, J. E., Grätzel, M., Klug, D. R. & Durrant, J. R. Subpicosecond interfacial charge separation in dye-sensitized nanocrystalline titanium dioxide films. *J. Phys. Chem.* **100,** 20056–20062 (1996).
94. Haque, S. A. *et al.* Parameters influencing charge recombination kinetics in dye-sensitized nanocrystalline titanium dioxide films. *J. Phys. Chem. B* **104,** 538–547 (2000).
95. Ardo, S. & Meyer, G. J. Photodriven heterogeneous charge transfer with transition-metal compounds anchored to TiO_2 semiconductor surfaces. *Chem. Soc. Rev.* **38,** 115–164 (2009).
96. Dare-Edwards, M. P., Goodenough, J. B., Hamnett, A. & Trevellick, P. R. Electrochemistry and photoelectrochemistry of iron(III) oxide. *J. Chem. Soc. Faraday Trans.* **179,** 2027–2041 (1983).
97. Hanna, M. C. & Nozik, A. J. Solar conversion efficiency of photovoltaic and photoelectrolysis cells with carrier multiplication absorbers. *J. Appl. Phys.* **100,** 074510 (2006).
98. Shockley, W. & Queisser, H. J. Detailed balance limit of efficiency of p–n junction solar cells. *J. Appl. Phys.* **32,** 510–519 (1961).
99. Chen, Z. *et al.* Accelerating materials development for photoelectrochemical hydrogen production: Standards for methods, definitions, and reporting protocols. *J. Mater. Res.* **25,** 3–16 (2010).
100. Ekins, P. *Hydrogen Energy* (Earthscan, 2010).

Acknowledgements

Y.T. acknowledges funding support from JST, PRESTO. L.V. acknowledges support from the International Research Center for Renewable Energy, State Key Laboratory of Multiphase Flow in Power Engineering, Xian Jiaotong University, the Thousand Talents plan and the National Natural Science Foundation of China (no. 51121092). J.R.D. acknowledges the EPSRC and European Research Council for funding. The authors thank J. Nolan and J. Fenn, Design and Production Educational Technology Advancement Group (EduTAG), RMIT University, for their support in the illustration of Fig. 5.

Author contributions

Y.T. and L.V. contributed equally to this work. J.R.D. wrote the section on charge carrier dynamics and assisted in drafting other aspects of the manuscript. Y.T. organized the submission.

Competing financial interests

The authors declare no competing financial interests.